

AUTOGENOUS SELF-HEALING OF FIBRE CEMENTS

J Harris¹, Y Zhou¹, J Calabria-Holley¹, K Paine¹

1. University of Bath, UK

ABSTRACT. The University of Bath has developed innovative fibre cement capable of achieving flexural strengths in excess of 30 MPa. These fibre cements are manufactured by a bespoke method at a low water/cement ratio (less than 0.2). Consequently after hardening there is a considerable quantity of unhydrated cement (a quaternary blend of Portland cement-fly ash-silica fume and limestone) left in the paste. As a result of this it has been considered that after cracking these fibre cements will have significant potential for autogenous healing primarily as a consequence of the hydration of this unhydrated cement and associated pozzolanic reactions. This paper reports on research carried out to test this hypothesis. A number of fibre cements were cast and then cracked after 28 days of curing. The fibre cements were then subject to a number of healing regimes. It was shown that substantial post-crack healing did occur in fibre cements; conventional fibre cements cast at a higher w/c ratio (0.5) were shown not to heal. The precise mechanism of healing was, however, less clear and appears to be due to the leaching of calcium hydroxide and its subsequent carbonation rather than delayed hydration. Reasons for this are discussed in the paper.

Keywords: Cracks, Fibre Cements, Self-healing, Hydration, Carbonation

Mr Jack Harris was an undergraduate student in the Department of Architecture and Civil Engineering at the University of Bath. He graduated with a MEng in civil engineering in 2018.

Mr Yanjun Zhou was a postgraduate student in the Department of Architecture and Civil Engineering at the University of Bath. He graduated with a MSc in civil engineering: innovative structural materials in 2017.

Dr Juliana Calabria-Holley is a Lecturer in the BRE Centre for Innovative Construction Materials at the University of Bath. Her research focuses on nanotechnology to improve building materials performance.

Dr Kevin Paine is a Reader and Deputy Director of the BRE Centre Innovative Construction Materials at the University of Bath. His research focuses on smart concrete technologies.

INTRODUCTION

Fibre cement is widely used for the production of exterior and interior protective surfaces. It is manufactured by carefully engineering the inclusion of polyvinyl alcohol (PVA), and sometimes cellulose, fibres into a cementitious matrix. The matrix itself only contains powder materials of which cement is the principal product [1]. Fibre cements are normally manufactured using the Hatschek process which generates a pliable material that can be moulded into a variety of shapes, although for laboratory purposes alternative manufacturing methods can be used [2]. Fibre cement is resilient, light but exceptionally strong in flexure.

As part of an EU funded project in collaboration with the Danish fibre cement manufacturer Cembrit, the University of Bath has developed innovative fibre cement capable of achieving flexural strengths in excess of 30 MPa. These fibre cements are manufactured by a bespoke method at a low water/cement ratio (less than 0.2). Because of the low w/c ratio after hardening there is a considerable quantity of unreacted cementitious material left in the paste. As a result of this it has been considered that after cracking these fibre cements will have significant potential for autogenous healing as a consequence of the later hydration of this unhydrated cement and associated pozzolanic reactions.

The ability of early-age cementitious materials to undergo autogenous healing is well known. Typically small cracks of a maximum size of 150 μm [3] can be healed due to the chemical processes associated with: (i) continued hydration of cement and (ii) carbonation of calcium ions in the cement matrix due to ingress of carbon dioxide [4]. In addition to these chemical processes, it has been suggested that physical processes, such as swelling, and mechanical processes related to debris within the crack can contribute to autogenous healing [5].

The ability of fibre cements to self-heal through autogenous means may be similar to that observed in engineered cementitious composites (ECC) [6]. ECCs are high performance ductile materials which typically contain 2% fibres by volume. During deformation ECCs can maintain a crack width of 60 μm up to failure. This tendency to form small cracks is due to the concrete's ability to experience "flat crack propagation", whereby the width of the crack remains constant but the length may increase indefinitely. This makes ECCs ideal for autogenous healing as the crack width parameter has the most influence on concrete's ability to heal.

The aim of this research was to investigate whether the quantity of unhydrated cement left in these low w/c ratio fibre cement pastes could be utilised as a means of providing autogenous healing in the form of calcium silicate hydrate (C-S-H).

MATERIALS AND TESTING

Materials

The materials used were: Portland cement, (CEMI) conforming to BS EN 197-1. Silica fume conforming to BS EN 13263:2005 with a mean size of 0.15 μm [7]. Fly ash conforming to BS EN 450-1:2012 with a mean diameter of 9.1 μm . According to the manufacturer the oxide composition was SiO₂ 53.5%, Al₂O₃ 34.3%, Fe₂O₃ 3.6% and CaO 4.4% [8] and 4mm long PVA fibres (Kuralon H-1). The superplasticizer used was ViscoCrete 20 HE provided by Sika.

Mix proportions

Two types of fibre cements were investigated as shown in Table 1. The fibre cement of interest had a w/c ratio of 0.14 where the cement component (c) consists of a ternary blend of CEM I, silica fume and fly ash. For comparison fibre cement with a w/c ratio of 0.45 was also investigated. A total of 15 specimens with w/c = 0.14 were created and three specimens with w/c = 0.45. All specimens had dimensions of 120x40x10mm.

Table 1 Mix proportions (in g) for 1kg of fibre cement

w/c ratio	CEM I	SILICA FUME	FLY ASH	PVA FIBRES	SUPER-PLASTICISER	WATER
0.14	593	170	85	17	17	118
0.45	476	136	68	14	0	306

Mixing

Due to the low water cement ratio, w/c = 0.14 specimens were manufactured in a bespoke manner. Dry materials were first mixed by hand and then transferred to a shear mixer. The water and super plasticiser were then added and mixed thoroughly to ensure no dry powder remained. Once the paste had become a liquid the PVA fibres were added and the level of mixing energy reduced to prevent damage to the fibres.

The resulting mix was then transferred to a damp paper towel and covered to prevent drying out. Due to the low w/c ratio there was limited time available to cast samples as the water released by the shear mixing could quickly reabsorb into the paste. The samples were cast into 120x40x10mm moulds in lightly compacted layers, and finally subject to a pressure of 0.05 N/mm² for one minute. The moulds were placed in a sealed bag for 24 hours. After demoulding they were cured in water at 60°C for 1 week. After 1 week the samples were oven dried at 105°C for 24 hours to provide uniform moisture content for permeability testing prior to cracking.

w/c = 0.45 specimens were mixed using a conventional mortar mixer conforming to BS EN 196-1. They were compacted into the moulds in two layers but did not require a compaction pressure.

Tests methods

Permeability

Permeability testing was performed using 300mm long PVC tubes with an internal diameter of 20mm. The tubes were attached to the samples using silicon sealant at the centre point where cracks were designed to form (Figure 1). The tube was then filled with water to a height of 250 mm. Control tests were also carried out on a tube attached to a sheet of acrylic, to account for evaporation over the duration of the test. The samples were left for 24 hours and the change in water height was measured. The loss of water (minus that assumed to be due to evaporation) was taken as the permeability.



Figure 1 Permeability testing of fibre cements

After the tubes were detached, the silicon left on the samples was removed using water and emery paper.

Cracking

Sample cracking was carried out under three-point bending in conjunction with a crack mouth opening displacement (CMOD) gauge to measure lateral displacement. The specimens were loaded to obtain cracks of between 50 and 200 μm in width (after unloading). Following cracking a further permeability test was performed on all the samples

Healing conditions

The cracked specimens were placed in a water bath with the crack face up to allow water to enter the crack freely. Water baths were set at 20°C. The samples were left for one week before they were removed and examined for healing (Figure 2).



Figure 2: Cracked fibre cement specimens placed in a water bath to heal

Detection of healing

After one week the samples were removed from the water bath and dried to permit initial non-intrusive investigations both by eye and via microscopy. The crack width was measured to determine the degree of crack healing. A third and final permeability test was carried out to deduce if there had been a reduction in permeability that could be attributed to healing of the samples.

The final stage of testing involved invasive investigation via scanning electron microscopy (SEM). Two samples were chosen, one that appeared to have healed and one where the crack remained visible. Both samples were initially cast in resin whilst being evacuated in a vacuum to remove any air from both sample and resin. The initial cast in resin was done to support the samples during cutting and prevent unintentional damage. Samples were then cut to extract the centre containing the crack. They were then cut again this time perpendicular to the crack so a section of the fracture for examination. The dissected pieces were then recast in resin and their surface of interest polished ready for investigation using SEM.

RESULTS

Cracking

The crack widths generated are given in Table 2. It can be seen that a wide range of crack widths, from 70 to 200 μm , were generated as intended. This provided for the capability to examine the autogenous healing of a range of cracks. The crack widths generated for the $w/c = 0.45$ specimens were lower than the $w/c = 0.14$ specimens and ranged from 40 to 75 μm .

Visual crack healing

After the one week healing period samples were re-examined to discover if any visual difference in crack morphology could be detected.

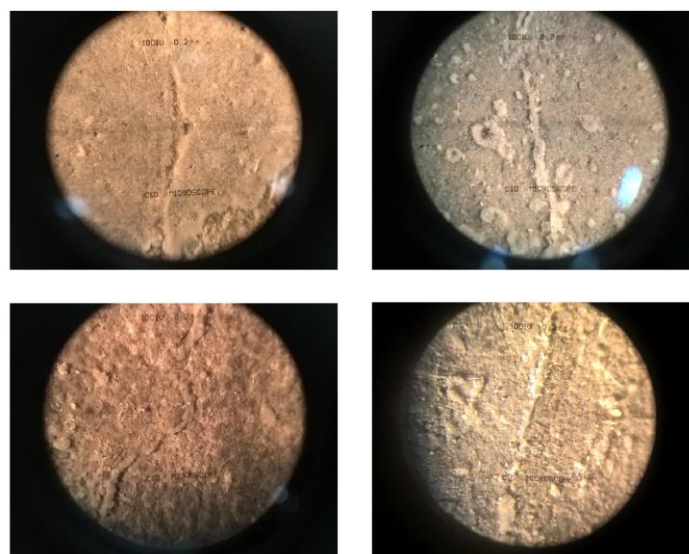


Figure 3: Healing of selected $w/c=0.14$ specimens after 1 week

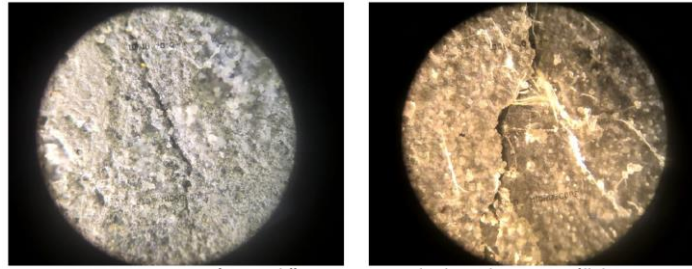


Figure 4: Incomplete healing of w/c = 0.45 specimens after 1 week

It was found that for the w/c = 0.14 specimens there was a noticeable difference in crack size even without the need for a microscope and that in most cases the surface of the crack was filled with a healing compound (Figure 3). However, the healing product for w/c = 0.14 was not always uniform and in some cases, particularly for the larger cracks, only partial healing could be observed. It is possible that had the specimens had longer to heal then more extensive healing could have occurred thus increasing the homogeneity of product location. In contrast, the w/c = 0.45 specimens showed little surface healing despite having smaller crack widths (Figure 4).

Permeability

The initial permeability of all specimens before cracking, after cracking and after healing are given in Table 2. The initial permeability of all specimens was low, as expected, due to the small capillary pore size relating to the low w/c.

Table 2 Crack widths and water retention capability of specimens before cracking, after cracking and after healing

SPECIMEN	CRACK WIDTH, μm	WATER RETENTION, mm		
		Initial	cracked	healed
0.14-1	130	249	116	136
0.14-2	110	247	92	119
0.14-3	100	246	62	157
0.14-4	100	250	0	0
0.14-5	200	54	Not tested/damaged	
0.14-6	80	250	0	0
0.14-7	190	249	0	0
0.14-8	110	249	0	0
0.14-9	70	248	0	34
0.14-10	80	250	41	125
0.14-11	120	250	0	0
0.14-12	120	248	0	0
0.14-13	100	247	0	0
0.14-14	100	250	0	0
0.14-15	80	250	86	35
0.45-1	65	247	0	0
0.45-2	75	248	0	0
0.45-3	40	247	0	0

All specimens with the exception of 0.14-5 retained their water within appropriate limits. Sample 0.14-5 was damaged and leaked through a fissure. This specimen was not used in subsequent tests. There was no significant difference between the permeability of the $w/c = 0.14$ and $w/c = 0.45$ specimens.

The cracking of the specimens generated cracks that in most cases were sufficient to permit complete loss of water from the tubes during the test. However, five specimens with $w/c = 0.14$ did retain some water. This can be attributed to unforeseen blockages such as crack narrowing or debris from the testing phase obscuring the passage of water. This in itself can be considered a form of autogenous healing as described earlier. All losses of water recorded were noted to be due to flow of water through the cracks as no water was observed on the surface, i.e. there were no failures in the seal between tube and specimen.

The results of the water retention of the $w/c = 0.14$ specimens after healing are interesting. It appears that in some specimens there was an improvement in water retention. This was particularly the case where the specimen had shown some water retention capability after cracking. Specimen 0.14-9, which had a small initial crack size, improved in water retention. Other specimens, of larger size, showed no improvement in water retention suggesting that cracks had not sealed completely. A relationship between water loss and initial crack width is shown in Figure 5, but it was not possible to determine whether there was a maximum crack width that could be healed.

All $w/c = 0.45$ specimens showed complete loss of water despite the smaller initial crack widths. This suggests that no healing has taken place as evidenced by visual healing.

Analysis of Healing Material

The composition of the healing material was investigated more thoroughly using scanning electron microscopy (SEM) and energy-dispersive X-ray spectroscopy (EDX). The samples examined were 0.14-4 which did not show any improvement during the permeability test and 0.14-9 which demonstrated an ability to prevent water flow after healing. Single point EDX spectral analyses as well as element mapping to show changes in elemental quantities across a defined axis were used and electron microscope images were taken with samples being both uncoated and coated in gold to give elemental contrast and higher quality images respectively.

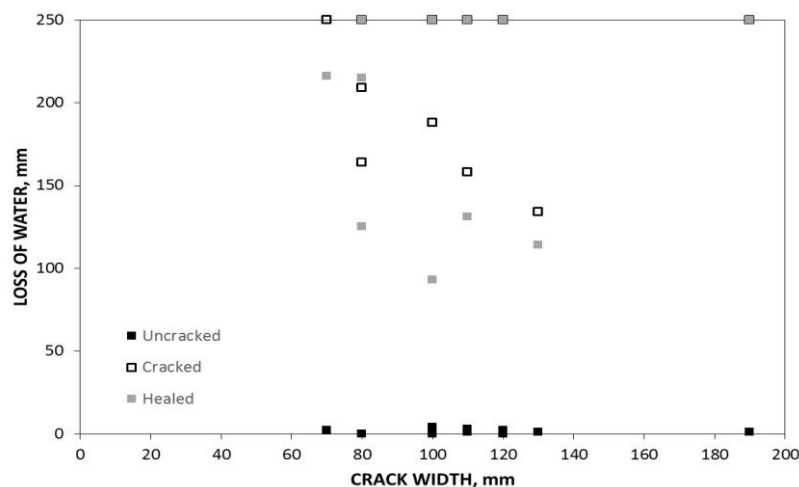


Figure 5 Relationship between loss of water and initial crack width

Figure 6 shows a SEM image of the healing product on the internal crack face of specimen 0.14-4. The elemental mapping carried out using SEM with EDS shows that this material has a high relative concentration of calcium. Whilst silicon is uniform in the bulk hardened cement paste it appears to be largely absent in the healing product. Furthermore, Figure 6,c?) shows a negligible amount of carbon in area identified as the healing product. Instead the carbon is present as a negative of the cement, this is due to the detector picking up the carbon in the resin used to contain the sample and subsequently fill the specimen voids. These maps therefore suggest that the healing product does not contain substantial quantities of silicon or carbon, leading to the conclusion the healing material is another compound of calcium. The most likely of which would be $\text{Ca}(\text{OH})_2$. However, as $\text{Ca}(\text{OH})_2$ is a by-product of cement hydration it is surprising that there is no presence of C-S-H in the healing product.

Figure 7 shows a map profile across the healing product that accumulated at the mouth of the crack in specimen 0.14-9. Note that this specimen showed no immediate post-crack water retention and consequently it is likely that this product only formed during the healing period. It can be seen that the calcium concentration is significantly raised in the healing product when compared to the original hardened cement paste, this concurs with the element mapping on 0.14-5 in Figure 6. The levels of silicon appear to be the inverse of the calcium and drop significantly when being measured in the healing product. Furthermore, there was no change in carbon. In addition, Figure 7 shows the level of aluminium and confirms that the healing product is not a form of calcium aluminate hydrate (C-A-H). Whilst map profiles do not show the physical quantity of each element, but merely the relationship of concentrations across a one dimensional slice, the exact chemical composition of the healing product cannot be determined. However, the evidence again suggests that the healing product is $\text{Ca}(\text{OH})_2$.

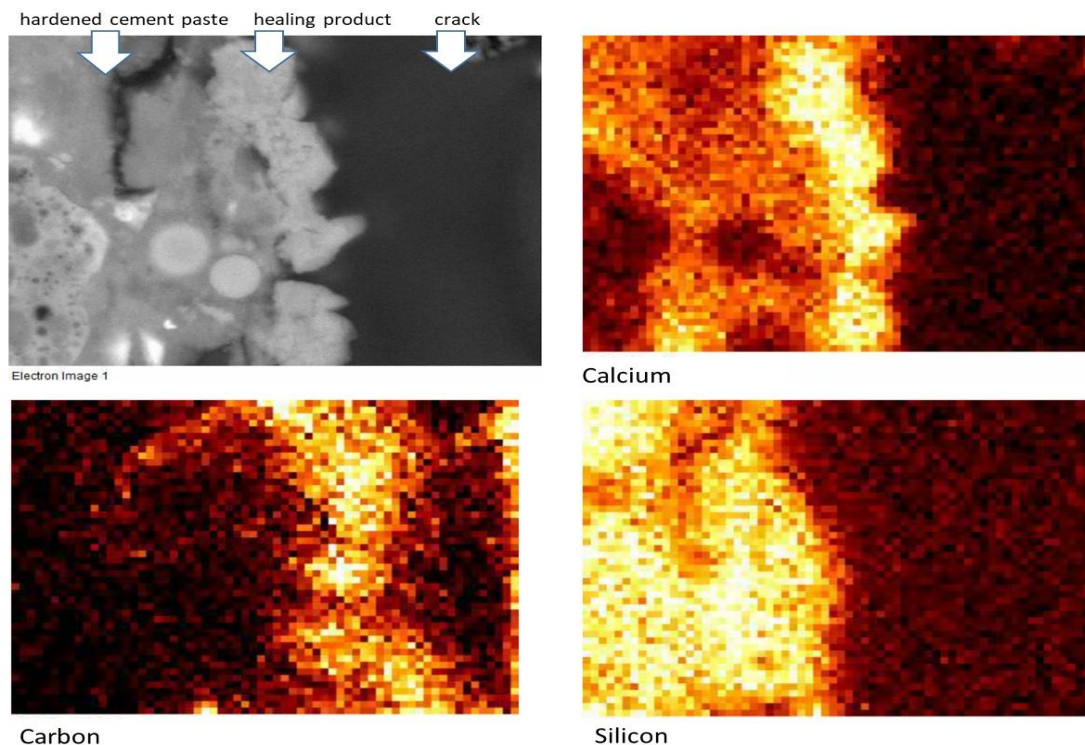


Figure 6 Element mapping of the initial hardened cement paste, healing product and crack showing the concentrations of calcium, carbon and silicon (The brighter the image the higher the concentration of a given element).

Towards the end of the imaging, it was noticed in several areas where healing product had formed that there was a difference in tone within the healing product itself. The images relayed to the monitor showed black and white images with lighter areas representing heavier compounds and vice versa for the darker areas. If the healing product was a homogenous lattice of $\text{Ca}(\text{OH})_2$ then the image should be of a uniform brightness however, by increasing images contrast it becomes more apparent that this was not the case. Material located at the fringes of the healing product was brighter and therefore represented a heavier compound. One such heavier species and therefore potential candidate for this material is C-S-H.

DISCUSSION

As no sample achieved its original permeability it can be concluded that complete healing did not occur and that a longer healing period should have been utilised. The decision to only allow the samples to heal for one week was based on the hypothesis that healing would occur due to reactions between ingressing water and unhydrated cement in the low w/c ratio fibre cements. Whilst this hypothesis appears to be true the indication that the healing product was primarily $\text{Ca}(\text{OH})_2$ rather than C-S-H was unexpected.

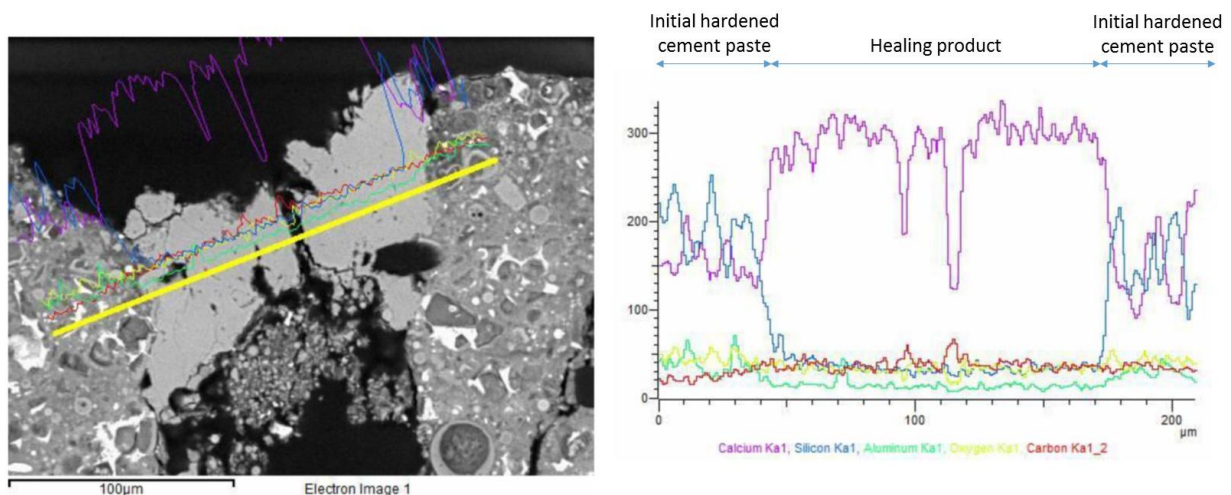


Figure 7 Element map profile of 0.14-9 at the crack mouth location

However, it appears that this finding is consistent with other research. For example, Huang et al [4,9] carried out research to investigate the autogenous self-healing of cement pastes at $w/c = 0.3$. Again it was expected that the C-S-H would be the main healing compound. However, they observed that the healing product comprised of 78% $\text{Ca}(\text{OH})_2$ and 17% C-S-H. Like our research the healing product differed substantially from the composition of the original bulk hardened cement paste.

Unlike C-S-H, $\text{Ca}(\text{OH})_2$ is not an ideal product for providing self-healing of concrete. Consequently, it is unsurprising that the water retention recovery was poor. However, given favourable conditions it is likely that this $\text{Ca}(\text{OH})_2$ would carbonate into CaCO_3 which is much more efficient for crack-sealing [10]. Indeed, some later microscopy tests carried out on specimens coated in gold to improve image resolution revealed compounds that were morphologically closer to CaCO_3 than $\text{Ca}(\text{OH})_2$ suggesting that this process was under way

once the specimens had been removed from the water bath. Consequently, in future tests we must allow for carbonation of the $\text{Ca}(\text{OH})_2$ before proceeding with tests on “healed” materials. It is also possible that the presence of $\text{Ca}(\text{OH})_2$ could lead to pozzolanic reactions with unhydrated silica fume and fly ash to create C-S-H.

CONCLUSIONS

The research has shown that fibre cements with low w/c ratio have greater capacity to autogenously self-heal than fibre cements of higher w/c ratio. Whilst w/c = 0.14 specimens visually showed complete or partial closure of cracks, no w/c = 0.45 samples provided any visual evidence of self-healing. Permeability tests showed that some w/c = 0.14 specimens could provide resistance to water flow after only one week of healing. No recovery in water retention was observed in the w/c = 0.45 specimens despite smaller initial crack widths.

Through SEM and other microscopic analysis the healing product was observed to comprise of calcium but contain little silicon or carbon. Consequently, it appears that $\text{Ca}(\text{OH})_2$ is the main healing product. It is probable that this $\text{Ca}(\text{OH})_2$ will later carbonate to form CaCO_3 providing an effective healing product, but this needs to be confirmed.

The study has shown that although the healing mechanism was not quite as hypothesised, fibre cements produced at low w/c ratios have unreacted material present that is capable of hydrating to form a healing product, albeit primarily $\text{Ca}(\text{OH})_2$ rather than C-S-H. Consequently, fibre cements at low w/c ratios have greater capacity for autogenous healing than fibre cements made at higher w/c ratios.

ACKNOWLEDGMENTS

The low w/c ratio fibre cements used in this study were developed as part of a European Commission FP7 funded project (FIBCEM, grant number 262954) and JCH and KP wish to thank our partners on that project, particularly Jacob Lund at Cembrit. KP acknowledges the contribution of the EPSRC funded programme grant (Project number EP/PO2081X/1), Resilient Materials for Life (RM4L).

REFERENCES

1. VAN DER HEYDEN L. Technical specifications of matrix raw materials for Hatschek technology based fibrecement – A pragmatic approach. *Constr Build Mater.* 2010;24(2):147-157.
2. AKHAVAN A, CATCHMARK J, RAJABIPOUR F. Ductility enhancement of autoclaved cellulose fiber reinforced cement boards manufactured using a laboratory method simulating the Hatschek process. *Constr Build Mater.* 2017;135:251-259. doi:10.1016/J.CONBUILDMAT.2017.01.001
3. AL-TABBAA A, LARK B, PAINE K, et al. Biomimetic cementitious construction materials for next-generation infrastructure. *Proc Inst Civ Eng – Smart Infrastruct*

- Constr. 2018;1-10. doi:<https://doi.org/10.1680/jsmic.18.00005>
4. DE BELIE N, GRUYAERT E, AL-TABBAA A, et al. A Review of Self-Healing Concrete for Damage Management of Structures. *Adv Mater Interfaces*. 2018;5(17):1-28.
 5. DE ROOIJ M, VAN TITTELBOOM K, DE BELIE N, SCHLANGEN E. Self-healing phenomena in cement-based materials. *RILEM State-of-the-Art Reports*. 2013;11.
 6. YANG Y, LEPECH MD, YANG E-H, LI VC. Autogenous healing of engineered cementitious composites under wet–dry cycles. *Cem Concr Res*. 2009;39(5):382-390.
 7. CALABRIA-HOLLEY J, PAINE K, PAPATZANI S. Effects of nanosilica on the calcium silicate hydrates in Portland cement–fly ash systems. *Adv Cem Res*. 2015;27(4):187-200.
 8. PAPATZANI S, PAINE K. Polycarboxylate/nanosilica-modified quaternary cement formulations – enhancements and limitations. *Adv Cem Res*. 2017;30:1-14.
 9. HUANG H, YE G, DAMIDOT D. Effect of blast furnace slag on self-healing of microcracks in cementitious materials. *Cem Concr Res*. 2014;60:68-82.
 10. VAN TITTELBOOM K, DE BELIE N. Self-healing in cementitious materials-a review. *Materials (Basel)*. 2013;6(6):2182-2217